Robust feedback controller in finite frequency based on H∞ performance for a variable speed wind turbine

Youssef Berrada* and Ismail Boumhidi

LESSI Laboratory,
Physics Department,
Faculty of Sciences,
Sidi Mohamed Ben Abdellah University,
B.P.1796 Fez-Atlas, 30003, Morocco
Email: youssef.berrada@usmba.ac.ma
Email: ismail.boumhidi@usmba.ac.ma
*Corresponding author

Abstract: The modern wind turbine system is modelled as a flexible structure operating in the presence of wind speed turbulences. Furthermore, it's highly nonlinear and its dynamic changes rapidly with the change of wind speed. A sophisticated control system is needed to allow wind turbines to generate power in a wide variety of wind conditions. This paper investigates a system control in finite frequency based on H∞ performance in order to maximise the extracted energy from the wind while mitigating aerodynamic loads. The finite frequency approach is used to design a robust feedback control to stabilise the system when the disturbances occur in a finite frequency band due to the stochastic nature of the wind flow. The controller gains are given in terms of linear matrices inequality (LMIs) which can be solved easily using existing numerical tools. The performance of the proposed control strategy is investigated in terms of stability and robustness under variable wind speed, and illustrated by tests simulation using MATLAB® software.

Keywords: finite frequency; H∞ performance; variable speed wind turbine.

Reference to this paper should be made as follows: Berrada, Y. and Boumhidi, I. (2021) 'Robust feedback controller in finite frequency based on H∞ performance for a variable speed wind turbine', *Int. J. Powertrains*, Vol. 10, No. 1, pp.104–123.

Biographical notes: Youssef Berrada received his PhD degree from Sidi Mohamed Ben Abdellah University in 2018, MSc in Signals, Systems and Computer from Faculty of Sciences, Fez Morocco in 2013 and BSc in Mechanical, Automation and Electro-Mechanics from Polydisciplinary Faculty Taza, Morocco in 2011. Currently, he is a researcher at Laboratory of Electronics, Signals, Systems and Informatics (LESSI), Physics Department, Faculty of Sciences Sidi Mohamed Ben Abdellah University. His research interests include modelling, control and optimisation of wind turbine energy conversion systems.

Ismail Boumhidi is a Professor of Electronic and Automatic at the Faculty of Sciences, Fez Morocco. He received his PhD degree from Sidi Mohamed Ben Abdellah University, Faculty of Sciences in 1994 and a state PhD degree in 1999. His research areas include adaptive and robust control, multivariable nonlinear systems, fuzzy logic control with applications and renewable energies.

1 Introduction

Since the oil crisis in the 1970s, global interest for clean and renewable energy sources has been increasing intensively. Wind energy has received a strong impulse; this reflected in great technology advances regarding reliability and cost-efficiency (Bakhshi and Sandborn, 2018). Control techniques have a major effect on the development of wind energy conversion systems, and remain a key factor for maximising the extracted energy from the wind and reducing the stresses caused by aerodynamic loads.

Recently, a number of control strategies have been developed and applied to wind energy systems such as a feedback linearisation control in which the nonlinearities of the system have been taken into account to achieve an optimal nonlinear controller over a variable speed range to maximise the power conversion of wind turbine (Yang et al., 2016), a nonlinear controller for a variable speed wind turbines with wind speed estimation have been addressed in Saravanakumar and Jena (2016), an adaptive pitch control with load mitigation capability has been studied to improve the lifetime of wind turbines operating in high wind speeds (Yuan and Tang, 2017), an optimal real-time controller has been developed to improve the performance of tracking the optimal tip speed ratio (Ma et al., 2015), a sliding mode control has been used to maximise the energy capture form the wind and to reduce the oscillatory behaviour of drive-trains (Mérida et al., 2014), a neural network sliding mode control have been synthesised for a wind turbine with uncertainties in real time (Berrada and Boumhidi, 2017), a predictive optimisation control based on neural network has been developed for large wind turbines (Han et al., 2017), also a predictive ramping control strategy for wind turbines with load reduction have been proposed in Liu et al. (2017). Yet, in most of these control techniques, the control law was implemented and tested under specific wind speeds. However, its performance is limited due to the stochastic nature of wind speed. For example, in the case of short and strong wind turbulences, turning off the wind turbines may not be the best solution for the safety of system equipment for two reasons: economic and environmental. Economically, the cost of energy to restart the wind farms, especially for medium and large size wind turbines. From the environmental perspective, the need for energy in isolated sites; where the wind farms are not connected to the grid to compensate the required energy. In addition, note that when the system disturbances occur within a finite frequency domain which be known beforehand, it is not favorable to investigate the system in the full frequency band, because this may introduce some conservatism and poor performance of system control.

Many important results in finite frequency domain have been investigated in the literature such as in Chibani et al. (2018a) the authors designed an observer in finite frequency for T-S fuzzy systems with unknown inputs. A fault detection filter is designed in Chibani et al. (2018b) for discrete-time polynomial fuzzy systems with faults and unknown disturbances while the frequency domains of the faults and the disturbances are assumed to be known beforehand and to reside in low, middle or high frequency ranges. The problem of state estimation of T-S fuzzy systems subject to unknown inputs by designing an observer in finite frequency domain is dealt in Chibani et al. (2016) to reduce the conservatism generated by those designed in the entire frequency domain when the unknown input frequency ranges are known beforehand. In Davoodi et al. (2019), a fault detection and isolation filter design in low frequency domain for discrete-time multi-agent LPV systems aiming at decreasing the conservatism of the entire frequency domain is investigated. A fuzzy filter designing for discrete-time nonlinear

systems in the Takagi Sugeno form is investigated in Ding and Yang (2010). The control problem in finite frequency domain has also been addressed in many research works, such as in Berrada et al. (2019). A feedback finite frequency Takagi-Sugeno (T-S) fuzzy controller is synthesised for a variable speed wind turbine. A finite frequency control is proposed in Berrada and Boumhidi (2018) to improve the sliding mode control for a wind turbine against a sudden fast change and fluctuation of wind speed. An adaptive mechanism is introduced in Li and Yang (2015) to construct a novel finite frequency H∞ controller with time-varying gains for uncertain linear systems. A robust finite frequency H∞ passive fault-tolerant static-output-feedback control is designed in Zhang et al. (2014). A problem of active fault-tolerant control in considered in Qiu et al. (2011) for vehicle active suspension systems in finite frequency range. The control synthesis is essentially based on the lemma of generalised-Kalman-Yakubovich-Popov (GKYP), which converts the different properties of the system dynamic in a finite frequency domain into LMI conditions (Iwasaki and Hara, 2005).

In this context, this article investigates a finite frequency nonlinear controller based on H∞ performance to maximise the energy extracted from the wind and attenuates the aerodynamic loads caused by large fluctuations in wind speed. The developed state feedback controller is applied to a wind turbine two-mass model which is a highly nonlinear model. The H∞ approach consists to ensure the stability of the closed-loop system with a certain degree of disturbances attenuation for the entire studied domain. The effectiveness of the H∞ controller in the wind energy control field has also been validated by many researchers (Menezes et al., 2018). A comparison between H∞ control and PID regulator established in Moradi and Vossoughi (2015) proved that both control strategies have the same performance regarding power extraction and another comparative study established in Young-Man (2016) has validated the performance of the H∞ control method compared to a LQG controller. But when the wind speed fluctuate rapidly within a short period; this controller may be destroyed. However, the finite frequency approach is able to retain almost all the robustness properties of the system over a specific frequency range, and then resolve this problem. The main purpose of this control is to obtain the maximum power extracted under fast turbulences of wind speed and to reduce the produced vibratory behavior of the control system. The control law is designed based on some useful Lemmas, where the control conditions are given in terms of linear matrices inequality (LMIs). And their effectiveness is evaluated using a FAST model based on the Controls Advanced Research Turbine parameters (Johnson and Fleming, 2011).

The rest of this manuscript is organised as follows: Section 2 describes the dynamic model of the wind turbine. Next, the design of the control technique is presented in Section 3. The simulation results are shown in Section 4. Finally, some conclusions are given in Section 5.

Notations: The superscript '^{T}' stands for matrix transposition. 'I' denotes an identity matrix with appropriate dimension, $diag\{\ldots\}$ stands for block diagonal matrix, $tr(A)$ denotes the trace of matrix A. The notations $A > 0$ and $A < 0$ mean that matrix A is positive definite and negative definite, respectively.

Nomenclature

Ω_r rotor speed [rad/s]

J_r rotor inertia [kg.m^2]

K_r rotor friction coefficient [N.m/rad/s]

θ_r rotor side angular deviation [rad]

T_{ls} shaft torque [N.m]

B_{ls} shaft stiffness coefficient [N.m/rad]

K_{ls} shaft damping coefficient [N.m/rad/s]

θ_{ls} gearbox side angular deviation [rad]

T_{hs} shaft torque [N.m]

T_{em} generator electromagnetic torque [N.m]

J_g generator inertia [kg.m^2]

Ω_g generator speed [rad/s]

K_g generator friction coefficient [N.m/rad/s]

Ω_g generator side angular deviation [rad]

f rotation frequency [Hz]

v wind speed [m/s]

ρ air density [kg.m^3]

n_g transmission ratio

R rotor radius [m]

P_a aerodynamic power [W]

T_a aerodynamic torque [N.m]

C_p power coefficient

C_q torque coefficient

β pitch angle

λ tip speed ratio.

2 Wind turbine modelling

2.1 Aerodynamic

Aerodynamic is a very important aspect of wind turbines. Blade aerodynamic forces produce shaft torque and subsequently rotation that converted into electrical energy using generators (Berrada, 2018). The wind speed fluctuation with height of blades is one of the causes of aerodynamic loads. However, the aerodynamic loads impose excessive stresses on turbine drive-trains and appreciably shorten the lifetime of the machine. In fact, if the wind turbine rotor turns too slowly, most of the wind will pass undisturbed through the

apertures between the blades with little power extraction. On the other hand, if the rotor turns too fast, the rotating blades act solid wall obstructing the wind flow again reducing the power extraction. Wind turbines must be controlled to operate at their optimal wind tip speed ratio in order to extract as much power as possible from the wind stream, at the same time, to mitigate aerodynamic loads that fatigue turbine components to extend the machine lifetime. The relationship between rotor speed and wind speed is defined by a ratio called tip speed (Wang et al., 2018)

$$Tip\ speed\ \ ratio: \lambda = \frac{tip\ speed\ of\ blade}{wind\ speed} = \frac{\Omega_r.R}{v} = \frac{2\pi f.R}{v} \tag{1}$$

Figure 1 Power coefficient $C_p(\lambda, \beta)$

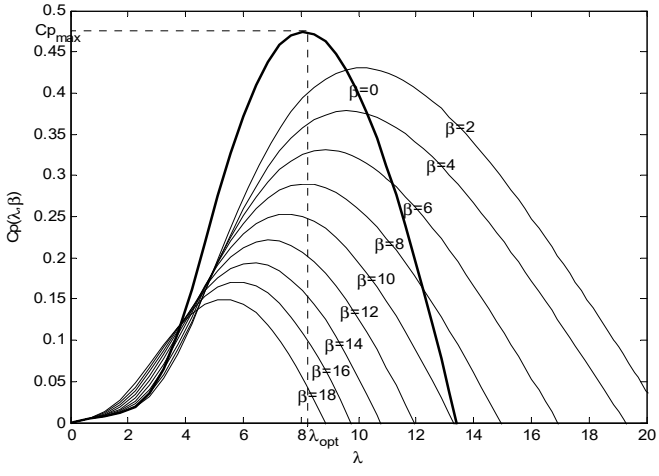

The aerodynamic power P_a extracted by the rotor is expressed as the following nonlinear expression (Berrada, 2018; Wang et al., 2018; Do et al., 2018)

$$P_a = \frac{1}{2}\rho\pi R^2 C_{p(}\lambda, \beta)v^3 \tag{2}$$

$C_P(\lambda, \beta)$ is the power coefficient depending nonlinearly upon the blade pitch angle and the tip speed ratio

$$C_P(\lambda, \beta) = c_1\left(c_2\lambda_i - c_3\beta - c_4\right)\times\exp\left(-c_5\lambda_i\right) + c_6\lambda \tag{3}$$

where $\lambda_i = \frac{c_7}{\lambda + c_8\beta} - \frac{c_9}{\beta^3 + c_{10}}$, and c_1 = 0.5109; c_2 = 116; c_3 = 0.4; c_4 = 5; c_5 = 21; c_6 = 0.0068; c_7 = 1; c_8 = 0.08; c_9 = 0.035; c_{10} = 1. The variation of the power coefficient depends on the pitch angle and the tip speed ratio is represented in Figure 1.

The aerodynamic power P_a is related to the aerodynamic torque T_a by:

$$P_a = T_a\Omega_r \tag{4}$$

Then the aerodynamic torque expression is:

$$T_a = \frac{1}{2}\rho\pi R^3 C_q(\lambda, \beta)v^2 \tag{5}$$

The torque T_a is a nonlinear function of rotor speed Ω_r (through λ), blade pitch angle β and the wind speed v. Where $C_q(\lambda, \beta)$ is the torque coefficient: $C_q(\lambda, \beta) = C_q(\lambda, \beta)/\lambda$.

2.2 Drive-trains

Drive-trains are a sequence of elements that transforms kinetic energy into electrical energy. The two-mass model is commonly used to model the dynamics of wind turbine drive-trains (Figure 2) (Berrada, 2018; Wang et al., 2018).

Figure 2 Two mass drive-trains model (see online version for colours)

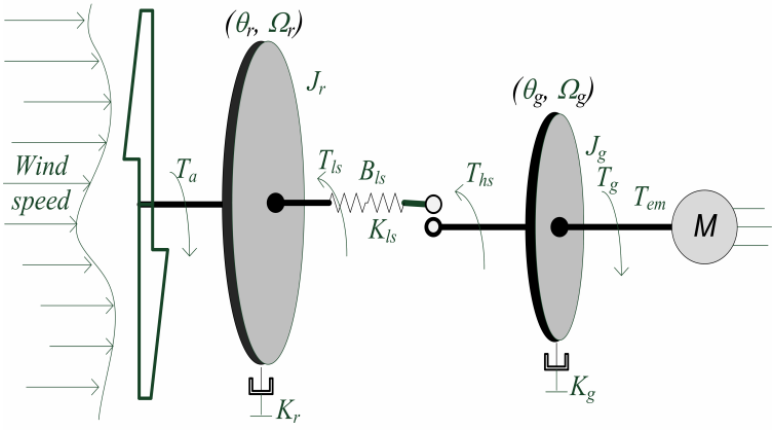

The dynamics of rotor speed Ω_r with rotor inertia J_r driven by aerodynamic torque T_a is characterised by the following differential equation:

$$J_r\dot{\Omega}_r = T_a - T_{ls} - K_r\Omega_r \tag{6}$$

Braking torque acting on the rotor is a low speed shaft torque T_{ls} which can be derived by using stiffness and damping factor of the low speed shaft

$$T_{ls} = B_{ls}(\theta_r - \theta_{ls}) + K_{ls}(\Omega_r - \Omega_{ls}) \tag{7}$$

The generator speed dynamics Ω_g with generator inertia J_g driven by the high speed shaft torque T_{hs} and broken by the electromagnetic torque T_{em} is given by:

$$J_g\dot{\Omega}_g = T_{hs} - K_g\Omega_g - T_{em} \tag{8}$$

The aim of the gearbox is to adapt the speed of rotation between the rotor and the generator. For an ideal gearbox, the transmission ratio n_g is defined as (Berrada, 2018):

$$n_g = \frac{T_{ls}}{T_{hs}} = \frac{\Omega_g}{\Omega_{ls}} = \frac{\theta_g}{\theta_{ls}} \tag{9}$$

From equations (6)–(9) and replacing the time derivative of T_{ls} (see Appendix), we obtain the following dynamic model:

$$\begin{aligned}
\dot{\Omega}_r &= -\frac{K_r}{J_r}\Omega_r - \frac{1}{J_r}\mathrm{T}_{ls} + \frac{1}{J_r}T_a \\
\dot{\Omega}_g &= -\frac{K_g}{J_g}\Omega_g + \frac{1}{n_g J_g}T_{ls} - \frac{1}{J_g}T_{em} \\
\dot{T}_{ls} &= \left(B_{ls} - \frac{K_{ls}K_r}{J_r}\right)\Omega_r + \frac{1}{n_g}\left(\frac{K_{ls}K_g}{J_g} - B_{ls}\right)\Omega_g \\
&\quad -K_{ls}\left(\frac{J_r + n_g^2 J_g}{n_g^2 J_g J_r}\right)T_{ls} + \frac{K_{ls}}{J_r}T_a + \frac{K_{ls}}{n_g J_g}T_{em}
\end{aligned} \tag{10}$$

2.3 Control problem formulation

The operate area of a variable speed wind turbine can be divided into three zones. As displayed in Figure 3 (Berrada, 2018):

Figure 3 Extracted power curve (see online version for colours)

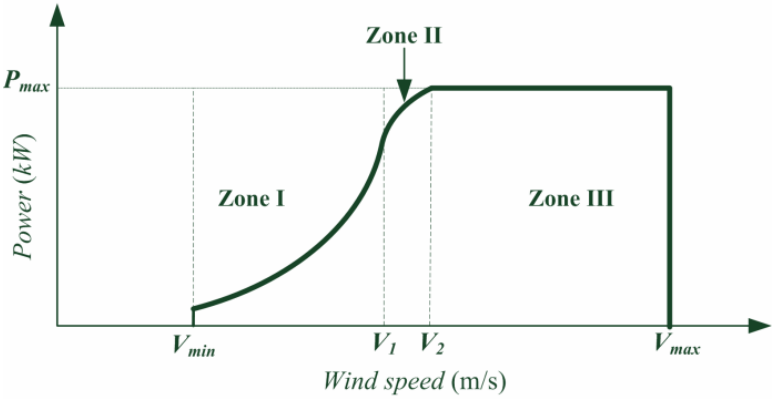

In zone I the wind turbine operates in partial loads, so the main control objective is to capture the maximum amount of power available in the wind. The power capture $C_p(\lambda, \beta)$ curve has a single maximum that corresponds to an optimal capture of the wind power $C_{p\max} = C_p(\lambda_{opt}, \beta_{opt})$ (see Figure 1). Consequently, in order to maximise the power extraction, the angle β should be fixed at its optimal value β_{opt}. The tip speed ratio λ (1) depends on both the wind speed and the rotor rotational speed, as the wind speed is a non-controllable input; the rotor speed must be adjusted to pursue the optimal reference given by:

$$\Omega_{r\,opt} = \frac{\lambda_{opt}}{R}v \tag{11}$$

Thus, the wind turbine model (10) becomes a single input single output system; the turbine rotor speed Ω_r and the electromagnetic torque T_{em} are respectively the output and the input of the system. In addition, we can obviously observe that this reference signal

(11) has the same form of wind speed v, so strong oscillations are generated when the wind speed is highly fluctuated. The control objective is then to track this reference, while trying to reduce the control oscillations and its effect of machine's drive-devices.

The other two zones (zones II and III) are not addressed in this work. These zones have already been considered in recent works (Berrada, 2018; Boukhezzar and Siguerdidjane, 2010). In zone II, the wind turbine operates in transient loads, the wind speed varying between low and high. The objective of control is therefore to stabilise the power production and to reduce the aerodynamic loads. This is generally achieved by using switching control strategies (Bououden et al., 2012; Cavanini et al., 2018). In zone III, the wind turbine operates in full loads. The control objective herein is to keep the output power constant at its rated value. This is generally achieved by keeping constant the generator torque and varying the pitch angle (Lahlou et al., 2019; Liu et al., 2016).

Figure 4 shows the simplified block-diagram of the control strategy.

Figure 4 Block-diagram of control strategy (see online version for colours)

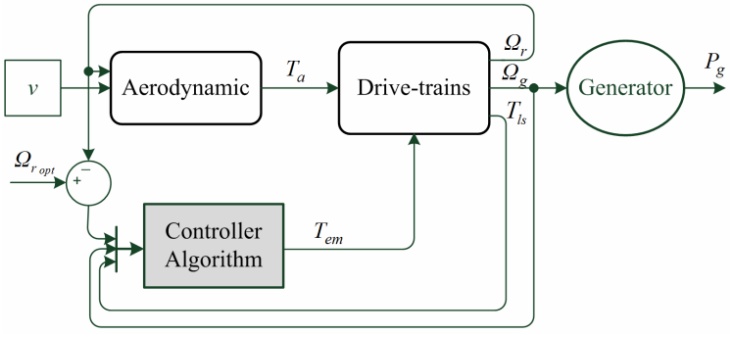

3 Control design

Let $E(t)$ be the tracking error defined by

$$E(t) = \Omega_{ropt}(t) - \Omega_r(t) \tag{12}$$

Below the rated power $\beta = \beta_{opt}$, then the state representation (10) can be reformulated as

$$\begin{aligned} \dot{x}(t) &= Ax(t) + Bu(t) + Dw(t) \\ y(t) &= Cx(t) \end{aligned} \tag{13}$$

where $x = [E\ \Omega_g\ T_{ls}]^T$, $y = E$, $u = T_{em}$, $w = [\Omega_{ropt} \quad \dot{\Omega}_{opt} \quad T_a]^T$ and the model matrices are

$$A = \begin{pmatrix} -\dfrac{K_r}{J_r} & 0 & \dfrac{1}{J_r} \\ 0 & -\dfrac{K_g}{J_g} & \dfrac{1}{n_g J_g} \\ -\left(B_{ls} - \dfrac{K_{ls}K_r}{J_r}\right) & \dfrac{1}{n_g}\left(\dfrac{K_{ls}K_g}{J_g} - B_{ls}\right) & -K_{ls}\left(\dfrac{J_r + n_g^2 J_g}{n_g^2 J_g J_r}\right) \end{pmatrix} \tag{14}$$

$$B = \begin{pmatrix} 0 \\ -\dfrac{1}{J_g} \\ \dfrac{K_{ls}}{ngJ_g} \end{pmatrix} \tag{15}$$

$$D = \begin{pmatrix} \dfrac{K_r}{J_r} & 1 & -\dfrac{1}{J_r} \\ 0 & 0 & 0 \\ \left(B_{ls} - \dfrac{K_{ls}K_r}{J_r}\right) & 0 & \dfrac{K_{ls}}{J_r} \end{pmatrix} \tag{16}$$

The state feedback control law is given by:

$$u(t) = Kx(t) \tag{17}$$

K is the state feedback gain. Combining (13) and (17) together, we can obtain the following closed loop system:

$$\begin{aligned} \dot{x}(t) &= A_c x(t) + Dw(t) \\ y(t) &= Cx(t) \end{aligned} \tag{18}$$

where $A_c = A + BK$. The transfer function from input $w(t)$ to output $y(t)$ is:

$$G(s) = C\left(sI - A_c\right)^{-1} D \tag{19}$$

Problem description: The objective is to design a state feedback controller (17) for the system (18) such that the following two conditions are satisfied:

1 The system (18) is asymptotically stable.

2 The system (18) is said to be a finite frequency H_∞ performance bound no larger than γ, if for the case of middle frequency the following inequality holds

$$\int_{\omega_1 \le \omega \le \omega_2} Y(\omega)^T Y(\omega) d\omega \le \gamma^2 \int_{\omega_1 \le \omega \le \omega_2} W(\omega)^T W(\omega) d\omega \tag{20}$$

where $\gamma > 0$ is a prescribed scalar and ω_1, ω_2 are the lower and upper limits of the concerned frequency domain, respectively. $Y(\omega)$ and $W(\omega)$ denote the Fourier transform of $y(t)$ and $w(t)$, respectively.

To design the controller, we introduce some basic lemmas, which will be used in the proof of our results.

Lemma 1. [Projection Lemma (Apkarian et al., 2001)] Given a symmetric matrix $\Psi \in \Re^{m \times m}$ and two matrices Γ, Π of column dimension m, there exists a matrix F such that the following LMI holds:

$$\Gamma F \Pi + \Pi^T F \Gamma^T + \Psi < 0 \tag{21}$$

If and only if the following projection inequalities with respect to F are satisfied:

$$\Gamma^{\perp}\Psi\Gamma^{\perp\mathrm{T}} < 0 \tag{22}$$

$$\Pi^{\perp}\Psi\Pi^{\perp\mathrm{T}} < 0 \tag{23}$$

where $\Gamma^{\perp}$ and $\prod^{\perp}$ are the orthogonal complement of Γ and $\prod$, respectively.

Lemma 2. Let $\gamma > 0$ be a given scalar. For the closed-loop system (18) is asymptotically stable, and the FF $H\infty$ (20) is satisfied, if there exists Hermitian matrices $P > 0$, $Q > 0$ such that:

$$\begin{bmatrix} A_c & D \\ I & 0 \end{bmatrix}^T \begin{bmatrix} -Q & P + j\omega_c Q \\ P - j\omega_c Q & -\omega_1\omega_2 Q \end{bmatrix} \begin{bmatrix} A_c & D \\ I & 0 \end{bmatrix} + \begin{bmatrix} C^{\mathrm{T}}C & 0 \\ 0 & -\gamma^2\mathrm{I} \end{bmatrix} < 0 \tag{24}$$

where $\omega_c = \dfrac{\omega_1 + \omega_2}{2}$.

Proof. First, suppose (24) holds. Post multiplying by $[x(t)^T\ w(t)^T]$ from the left and by its conjugate transpose from the right, we have:

$$\begin{aligned} &2\dot{x}(t)Px(t) - \dot{x}^T(t)Q\dot{x}(t) + j\omega_c\dot{x}^T(t)Qx(t) - j\omega_c x^T(t)Q\dot{x}(t) \\ &\quad - \omega_1\omega_2 x^T(t)Qx(t) + y^T(t)y(t) - \gamma^2 w^T(t)w(t) \le 0 \end{aligned} \tag{25}$$

Note that for any vectors ϕ andφ, the equality $\phi^T Q\varphi = tr(\varphi\phi^T Q)$ holds. Then (25) can be rewritten as:

$$\begin{aligned} &\frac{d\left(x(t)^T Px(t)\right)}{dt} + y(t)^T y(t) - \gamma^2 w(t)^T w(t) \\ &\qquad \le tr\left[He\left(\omega_1 x(t) + j\dot{x}(t)\right)\left(\omega_2 x(t) + j\dot{x}(t)\right)^T Q\right] \end{aligned} \tag{26}$$

Taking the integrating from $t = 0$ to ∞ using the stability property, we have:

$$x(\infty)^T Px(\infty) + \int_0^\infty y(t)^T y(t)dt - \gamma^2\int_0^\infty w(t)^T w(t)dt \le tr\left(He(S)Q\right) \tag{27}$$

where

$$S = \int_0^\infty \left(\omega_1 x(t) + j\dot{x}(t)\right)\left(\omega_2 x(t) + j\dot{x}(t)\right)^T dt \tag{28}$$

Note that $x(\infty)^T Px(\infty) \ge 0$ for $P > 0$, then we have

$$\int_0^\infty y(t)^T y(t)dt \le \gamma^2\int_0^\infty w(t)^T w(t)dt + tr(He(S)Q) \tag{29}$$

By the Parseval's theorem (Skelton and Iwasaki, 1998), we have

$$S = \frac{1}{2\pi}\int_{-\infty}^{+\infty}(\omega_1 - \omega)(\omega_2 - \omega)\,X(\omega)X(\omega)^T d\omega \tag{30}$$

$$\int_0^\infty y(t)^T y(t)dt = \frac{1}{2\pi}\int_{-\infty}^{+\infty} Y(\omega)^T Y(\omega)d\omega \tag{31}$$

$$\int_0^{\infty} w(t)^T w(t)dt = \frac{1}{2\pi}\int_{-\infty}^{+\infty} W(\omega)^T W(\omega)d\omega \tag{32}$$

Not that S is Hermitian, then $tr(He(S)Q) = tr(SQ)$ and hence (29) is equivalent to:

$$\int_{-\infty}^{+\infty} Y(\omega)^T Y(\omega)d\omega - \gamma^2 \int_{-\infty}^{+\infty} W(\omega)^T W(\omega)d\omega \le 2\pi tr(SQ) \tag{33}$$

Note that $\dot{X}^T QX \ge 0$ for $Q > 0$, and $(\omega_1 - \omega)$ $(\omega_2 - \omega)$ for the middle frequency case $\omega_1 \le \omega \le \omega_2$. Then we have:

$$\begin{aligned} 2\pi tr(SQ) &= \int_{\omega_1 \le \omega \le \omega_2} (\omega_1 - \omega)(\omega_2 - \omega) tr\left(XX^T Q\right) d\omega \\ &= \int_{\omega_1 \le \omega \le \omega_2} (\omega_1 - \omega)(\omega_2 - \omega) X^T QX d\omega \le 0 \end{aligned} \tag{34}$$

By (33) and (34) we have (20), and hence the finite frequency performance is satisfied.

Based on this lemma, an important theorem which can guarantee the asymptotic stability and the FF H∞ performance of the system (18) is going to be proposed.

Theorem 1. For a given constant $\gamma > 0$, consider the closed-loop system (18), if there exist matrices $\bar{Q} > 0$, $X > 0$, $Z > 0$ and general matrix Y, then the following LMIs are satisfied:

$$\begin{bmatrix} -\bar{Q} & -X + Z + j\omega_c \bar{Q} & 0 & 0 \\ * & AX + BY + XA^T + Y^T B^T - \omega_1\omega_2 \bar{Q} & D & XC^{\mathrm{T}} \\ * & * & -\gamma^2 I & 0 \\ * & * & * & -I \end{bmatrix} < 0 \tag{35}$$

$$AX^T + XA^T + BY + Y^T B^T < 0 \tag{36}$$

The state-feedback control gain K is given by:

$$K = YX^{-1} \tag{37}$$

Proof. Using Lemma 2, and according to the closed-loop system (18). The inequality (24) can be rewritten as:

$$\begin{bmatrix} A_C & D \\ I & 0 \\ 0 & I \end{bmatrix}^T \Psi \begin{bmatrix} A_C & D \\ I & 0 \\ 0 & I \end{bmatrix} < 0 \tag{38}$$

where

$$\Psi = \begin{bmatrix} -Q & P + j\omega_c Q & 0 \\ P - j\omega_c Q & \omega_1\omega_2 Q + C^{\mathrm{T}} C & 0 \\ 0 & 0 & -\gamma^2 I \end{bmatrix} \tag{39}$$

On the other hand we can write

$$\begin{bmatrix} I & 0 \\ 0 & 0 \\ 0 & I \end{bmatrix}^T \Psi \begin{bmatrix} I & 0 \\ 0 & 0 \\ 0 & I \end{bmatrix} = \begin{bmatrix} -Q & 0 \\ 0 & -\gamma^2 I \end{bmatrix} < 0 \tag{40}$$

By using the projection lemma (lemma 1), with

$$\begin{bmatrix} -I \\ A_c^T \\ D^T \end{bmatrix}^{\perp} = \begin{bmatrix} A_c^T & I & 0 \\ D^T & 0 & I \end{bmatrix} \tag{41}$$

$$\begin{bmatrix} 0 \\ \mathrm{I} \\ 0 \end{bmatrix}^{\perp} = \begin{bmatrix} \mathrm{I} & 0 & 0 \\ 0 & 0 & \mathrm{I} \end{bmatrix} \tag{42}$$

The following inequality is a sufficient condition for (24).

$$\Psi + \begin{bmatrix} -I \\ A_c^T \\ D^T \end{bmatrix} F [0 \quad \mathrm{I} \quad 0] + [0 \quad \mathrm{I} \quad 0]^T F \begin{bmatrix} -I \\ A_c^T \\ D^T \end{bmatrix}^T < 0 \tag{43}$$

This is equivalent to the following inequality (44).

$$\begin{bmatrix} -Q & -F + P + j\omega_c Q & 0 \\ * & A_c^* F + F A_c - \omega_1 \omega_2 Q + C^T C & FD \\ * & * & -\gamma^2 I \end{bmatrix} < 0 \tag{44}$$

By replacing $A_c = A + BK$ in (44) and performing the congruence transformation by $diag\{F^{-1} \quad F^{-1} \quad I\}$ and its transpose on the left and right, and further let $\bar{Q} = F^{-1} Q F^{-1}$, $X = F^{-1}$, $Z = F^{-1} P F^{-1}$, $Y = KF^{-1}$, then the inequality (44) can be rewritten as:

$$\begin{bmatrix} -\bar{Q} & -X + Z + j\omega_c \bar{Q} & 0 \\ * & AX + XA^T + BY + Y^T B^T - \omega_1 \omega_2 \bar{Q} + XC^T CX & D \\ * & * & -\gamma^2 I \end{bmatrix} < 0 \tag{45}$$

Applying the Schur complement to (44), we get exactly the inequality (35).

For the second sufficient condition of Theorem 1, let us construct a Lyapunov function inequality, A_c is stable if and only if there exists $F = F^T > 0$ such that

$$A_c^T F + F A_c < 0 \tag{46}$$

By substituting $A_c = A + BK$, we get

$$A^T F + K^T B^T F + FA + FBK < 0 \tag{47}$$

By multiplying both sides of (47) by the matrix F^{-1} and its transpose from the left and right, we can get

$$F^{-1}A^T + F^{-1}K^T B^T + AF^{-1} + BKF^{-1} < 0 \tag{48}$$

Let $X = F^{-1}$ and $Y = KF^{-1}$, then (48) became exactly the inequality (36). □

4 Simulation results

In this section, test simulations have been performed to show the performances of the proposed control approach (FF) compared to the control in the entire frequency domain (EF), and the PID controller which is widely used in the industry for wind energy systems (Menezes et al., 2018). The wind turbine with the characteristics in Table 1 and the drive-trains dynamics parameters listed in Table 2, is considered under a variable wind speed (Figure 5). The considered frequency domain represents the rotor operating frequency [0.9965 Hz 0.1939 Hz], which is calculated using (1) at the rated speed of rotor Ω_{ropt}.

Table 1 Wind turbine characteristics

Parameters	*Values*
Diameter of the rotor	43.3 m
Transmission ratio	43.165
Hub height	36.6 m
Nominal electrical power	600 Kw
Nominal rotor speed	42 tr/min
Maximum torque of generator	162 kN.m
Maximum rotor speed	53 tr/min
Maximum of the pitch angle	30°
Minimum of the pitch angle	–5°

Figure 5 Wind speed profile (see online version for colours)

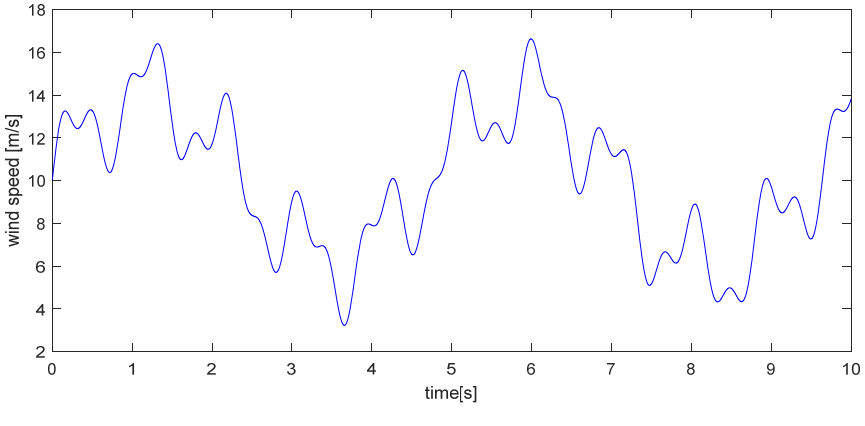

Table 2 Drive-trains parameters

Parameters	*Values*
ρ	1.29 kg/m^3
J_r	3.25×10^5 kg.m^2
J_g	34.4 kg.m^2
K_{ls}	9,500 N.m/rad/s
B_{ls}	2.691×10^5 N.m/rad
K_r	27.36 N.m/rad/s
K_g	0.2 N.m/rad/s

By solving Theorem 1 with the optimised parameter $\gamma > 0$, the control gains obtained from the two approaches are presented in Table 3.

Table 3 The obtained results from two methods controller

Control	*Gain (×10³)*	γ
FF	K= [294.6027 0.9989 –0.0135]	0.6912
EF	K= [566.2914 0.9738 –0.0077]	1.7646

The PID control gains are:

$$K_p = [5.2439 \;\; 0.5278 \;\; -0.000458] \times 10^5$$

$$K_i = [4.4939 \;\; 0.6745 \;\; -0.000458] \times 10^5$$

$$K_d = [2.9588 \;\; 0.2039 \;\; -0.000300] \times 10^2$$

In the first test, Figure 6 represents the time response of the rotor speed with FF, EF and PID controllers in red dotted line, blue dashed line and magenta dashdotted line respectively, and the black solid line represents the optimal signal, we can see obviously that the rotor speed controlled in finite frequency yields the best tracking.

Figure 6 Time response of rotor speed for the first test (see online version for colours)

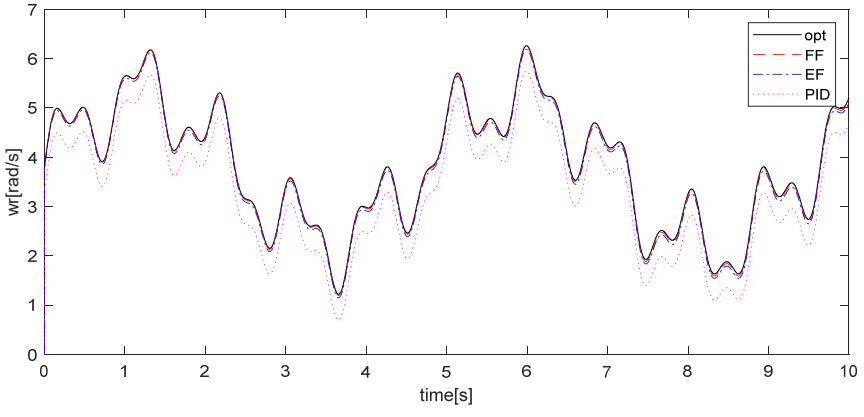

Figure 7 Time response of electromagnetic torque for the first test (see online version for colours)

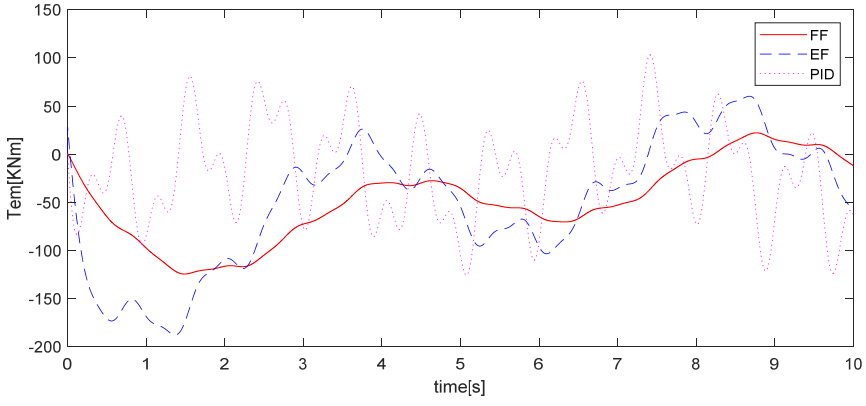

The pitch angle β is fixed at the optimal value and the rotor speed Ω_r is controlled by acting on the electromagnetic torque T_{em}, Figure 7 shows the torque variation T_{em} with FF in red solid line, EF in blue dashed line and PID in magenta dashdotted line, we can notice that the fluctuations of the proposed control law are less compared to the other controllers. And hence the aerodynamic loads are reduced.

In the second test, we increase the gains of PID by 10% compared to the first test, then the tracking is significantly improved (Figure 8, Figure 9), but the oscillations of control laws are increased (Figure 10), so these control strategies may therefore not be applicable because of the high oscillating behavior produced; and the override of the maximum value of the torque (162 kN.m, Table 1).

Figure 8 Time response of rotor speed for the second test (see online version for colours)

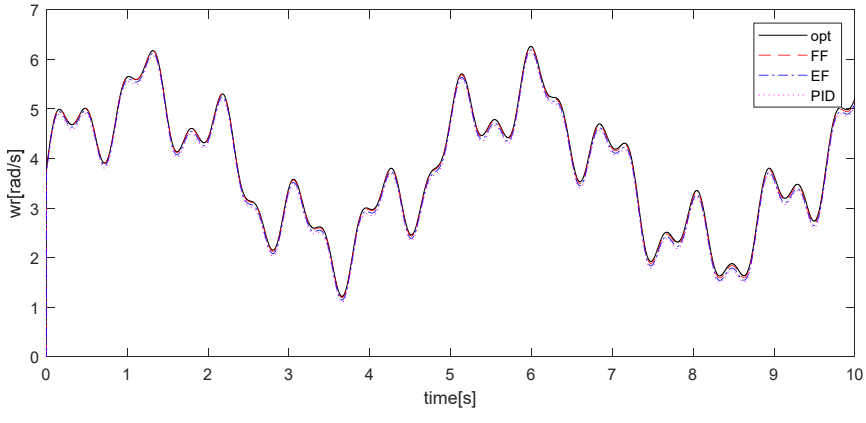

Figure 9 The zoom in portion of Time response of rotor speed for the second test (see online version for colours)

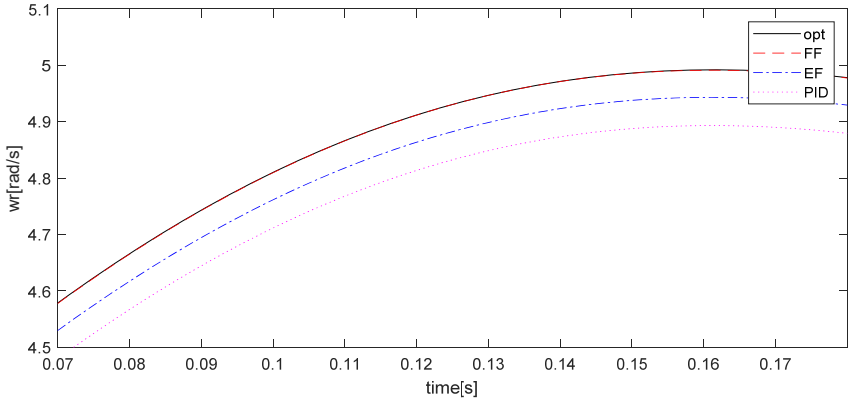

Figure 10 Time response of electromagnetic torque for the second test (see online version for colours)

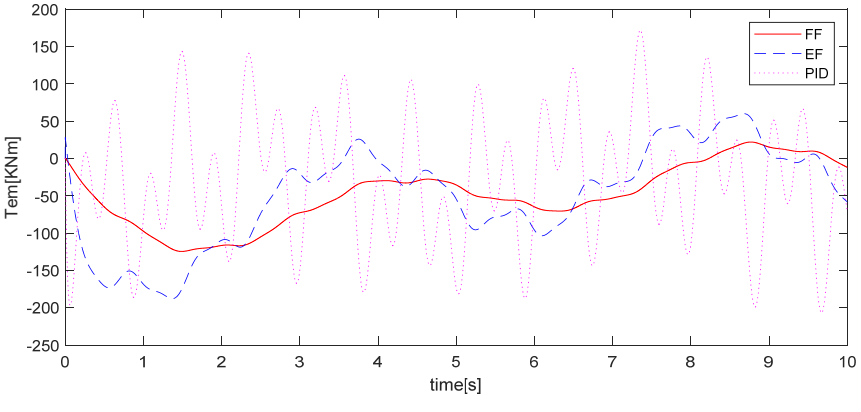

According to the results of the two tests, we can extract the following notes:

- The proposed control strategy achieves good tracking, and ensures the stability and robust performance of the system despite strong fluctuations of wind speeds. Consequently, the extracted wind energy is smoother and remains at its maximum value.
- The control efforts as well as the turbine stress are decreased compared to other approaches. Moreover, the implementation of the proposed control strategy leads to the more smooth behaviour of the control law (less vibration of actuators).
- Although the PID controller operates properly to track the optimal rotor speed by increasing control gains, this leads to unfavourable oscillatory behaviour in the control law and can be destroyed due to the high vibration of the actuators. This type of controller may be suitable for a fixed wind speed or a linear wind turbine Model.

Finally, we can draw that the proposed control strategy offers an interesting performance in terms of energy extraction and reduction of the behaviour of control oscillations caused by aerodynamic loads despite the turbulences of wind speed.

5 Conclusions

In this paper, a robust feedback controller in finite frequency based on H∞ performance is designed for a nonlinear model of the wind turbine aerodynamic under strong and fast wind fluctuations. The H∞ approach achieves the stability of the closed-loop system over the entire studied domain with a certain degree of disturbances attenuation, while the finite frequency approach is able to stabilise the system in a specific frequency range when the wind speed fluctuates rapidly. The control objective is to maximise the extracted wind power and to attenuate the aerodynamic loads. The controller conditions have been derived in terms of LMIs, which guarantee the stability of the closed-loop system. The performance of the proposed control strategy is investigated in terms of stability and robustness under variable wind speed and illustrated by simulation tests. This work will extend in the future for several wind turbine applications. Such as the fuzzy control and the fault tolerant control based on the finite frequency technique for variable speed wind turbine under great variety of wind conditions.

References

Apkarian, P., Tuan, H.D. and Bernussou, J. (2001) 'Continuous-time analysis, eigenstructure assignment, and H_2 synthesis with enhanced linear matrix inequalities (LMI) characterizations', *IEEE Trans. Autom. Control*, Vol. 42, No. 12, pp.1941–1946.

Bakhshi, R. and Sandborn, P.A. (2018) 'A return on investment model for the implementation of new technologies on wind turbines', *IEEE Transactions on Sustainable Energy*, Vol. 9, No. 1, pp.284–292.

Berrada, Y. (2018) *Modélisation, commande et optimisation d'un système éolien*, PhD thesis, Sidi Mohamed Ben Abdellah University, Fez Morocco.

Berrada, Y. and Boumhidi, I. (2017) 'Neural network sliding mode control with time-varying delay for a variable speed wind turbine', *International Journal of Power and Energy Conversion*, Vol. 8, No. 4, pp.343–356.

Berrada, Y. and Boumhidi, I. (2018) 'Sliding mode control for a wind turbine in finite frequency', *International Journal Engineering Systems Modelling and Simulation*, Vol. 10, No. 1, pp.39–48.

Berrada, Y., El Amrani, A. and Boumhidi, I. (2019) 'Feedback TS fuzzy controller in finite frequency for wind turbine,' *Modeling, Identification and Control Methods in Renewable Energy Systems*, pp.265–280, Springer, Singapore.

Boukhezzar, B. and Siguerdidjane, H., (2010) 'Nonlinear control of a variable-speed wind turbine using a two-mass model', *IEEE Trans. Energy Convers.*, Vol. 201, No. 26, No. 1, pp.149–162.

Bououden, S., Chadli, M., Filali, S. and El Hajjaji, A. (2012) 'Fuzzy model based multivariable predictive control of a variable speed wind turbine: LMI approach', *Renewable Energy*, Vol. 37, No. 1, pp.434–439.

Cavanini, L., Corradini, M.L., Ippoliti, G. and Orlando, G. (2018) 'A control strategy for variable-speed variable-pitch wind turbines within the regions of partial-and full-load operation without wind speed feedback', *2018 European Control Conference (ECC)*, IEEE, pp.410–415.

Chibani, A., Chadli, M. and Braiek, N.B. (2018a) 'Finite frequency observer design for T-S fuzzy systems with unknown inputs: an LMI approach', *Int. J. Modelling, Identification and Control*, Vol. 29, No. 2, pp.109–117.

Chibani, A., Chadli, M. and Braiek, N.B., (2016) 'A finite frequency approach to H∞ filtering for T–S fuzzy systems with unknown inputs', *Asian Journal of Control*, Vol. 18, No. 5, pp.1608–1618.

Chibani, A., Chadli, M., Ding, S.X. and Braiek, N.B. (2018b) 'Design of robust fuzzy fault detection filter for polynomial fuzzy systems with new finite frequency specifications', *Automatica*, Vol. 93, pp.42–54.

Davoodi, M., Chadli, M., Meskin, N. and Velni, J.M. (2019) 'Finite frequency fault diagnosis for heterogeneous multi-agent LPV systems', *2019 IEEE Conference on Control Technology and Applications (CCTA)*, IEEE, August, pp.1018–1023.

Ding, D.M and Yang, G.H. (2010) 'Fuzzy filter design for nonlinear systems in finite-frequency domain', *IEEE Trans. on Fuzzy Systems*, October, Vol. 18, No. 5, pp.935–945.

Do, H.T., Dang, T.D., Truong, H.V.A. and Ahn, K.K. (2018) 'Maximum power point tracking and output power control on pressure coupling wind energy conversion system', *IEEE Trans. Ind. Electron*., Vol. 65, No. 2, pp.1316–1324.

Han, B., Kong, X., Zhang, Z. and Zhou, L. (2017) 'Neural network model predictive control optimisation for large wind turbines', *IET Generation, Transmission & Distribution*, Vol. 11, No. 4, pp.3491–3498.

Iwasaki, T. and Hara, S. (2005) 'Generalized KYP Lemma: unified frequency domain inequalities with design applications', *IEEE Trans. Autom. Control*, Vol. 50, No. 1, pp.41–59.

Johnson, K.E. and Fleming, P.A. (2011) 'Development, implementation, and testing of fault detection strategies on the national wind technology center's controls advanced research turbines', *Mechatronics*, Vol. 21, Nos. , pp.728–736.

Lahlou, Z., Berrada, Y. and Boumhidi, I., (2019) 'Nonlinear feedback control for a complete wind energy conversion system', *International Review of Automatic Control (I.RE.A.CO.)*, Vol. 12, No. 3, pp.136–144.

Li, X.J. and Yang, G.H. (2015) 'Adaptive H∞ control in finite frequency domain for uncertain linear systems', *Information Sciences*, Vol. 314, No. 1, pp.14–27.

Liu, W., Li, C., Liu, Y. and Wu, Q. (2017) 'Predictive control of wind turbine for load reduction during ramping events', *International Journal of Electrical Power & Energy Systems*, Vol. 93, pp.135–145.

Liu, Y., Wu, Q.H. and Zhou, X.X. (2016) 'Co-ordinated multiloop switching control of DFIG for resilience enhancement of wind power penetrated power systems', *IEEE Transactions on Sustainable Energy*, Vol. 7, No. 3, pp.1089–1099.

Ma, Z., Yan, Z., Shaltout, M.L. and Chen, D. (2015) 'Optimal real-time control of wind turbine during partial load operation', *IEEE Transactions on Control Systems Technology*, Vol. 23, No. 6, pp.2216–2226.

Menezes, E.J.N., Araújo, A.M. and da Silva, N.S.B. (2018) 'A review on wind turbine control and its associated methods', *Journal of Cleaner Production*, Vol. 174, pp.945–953.

Mérida, J., Aguilar, L.T. and Dávila, J. (2014) 'Analysis and synthesis of sliding mode control for large scale variable speed wind turbine for power optimization', *Renewable Energy*, Vol. 71, pp.715–728.

Moradi, H. and Vossoughi, G. (2015) 'Robust control of the variable speed wind turbines in the presence of uncertainties: a comparison between H∞ and PID controllers', *Energy*, Vol. 90, No. 2, pp.1508–1521.

Qiu, J., Ren, M., Zhao, Y. and Guo, Y. (2011) 'Active fault-tolerant control for vehicle active suspension systems in finite-frequency domain', *IET Control Theory & Applications*, Vol. 5, No. 13, pp.1544–1550.

Saravanakumar, R. and Jena, D. (2016) 'Control strategy to maximize power extraction in wind turbine', *Distributed Generation & Alternative Energy Journal*, Vol. 31, No. 4, pp.27–49.

Skelton, R.E. and Iwasaki, T. (1998) *A Unified Algebraic Approach to Linear Control Design*, 285pp, Taylor and Francis, London, UK, ISBN0-7484-0592-5.

Wang, L., Cao, L. and Zhao, L. (2018) 'Non-linear tip speed ratio cascade control for variable speed high power wind turbines: a backstepping approach', *IET Renewable Power Generation*, Vol. 12, No. 8, pp.968–972.

Yang, B., Jiang, L., Wang, L., Yao, W. and Wu, Q.H. (2016) 'Nonlinear maximum power point tracking control and modal analysis of DFIG based wind turbine', *Journal of Electrical Power & Energy Systems*, Vol. 74, pp.429–436.

Young-Man, K. (2016) 'Robust data-driven H-infinity control for wind turbine', *Journal of the Franklin Institute*, Vol. 353, No. 13, pp.3104–3117.

Yuan, Y. and Tang, J. (2017) 'Adaptive pitch control of wind turbine for load mitigation under structural uncertainties', *Renewable Energy*, Vol. 105, pp.483–494.

Zhang, H., Wang, R., Wang, J. and Shi, Y. (2014) 'Robust finite frequency H∞ static-output-feedback control with application to vibration active control of structural systems', *Mechatronics*, Vol. 24, No. 4, pp.354–366.

Appendix

The shaft torque T_{ls} in (7) is a nonlinear function depending on rotor angular position θ_r, slow shaft angular position θ_{ls}, rotor speed Ω_r and slow shaft speed Ω_{ls}. The derivative of this torque with respect to time is the following:

$$\frac{dT_{ls}}{dt} = B_{ls}\left(\frac{d\theta_r}{dt} - \frac{d\theta_{ls}}{dt}\right) + K_{ls}\left(\frac{d\Omega_r}{dt} - \frac{d\Omega_{ls}}{dt}\right) \tag{49}$$

where

$$\frac{d\theta_r}{dt} = \Omega_r \tag{50}$$

$$\frac{d\theta_{ls}}{dt} = \Omega_{ls} \tag{51}$$

$$\frac{d\Omega_r}{dt} = \dot{\Omega}_r \tag{52}$$

$$\frac{d\Omega_{ls}}{dt} = \dot{\Omega}_{ls} \tag{53}$$

From the gearbox transmission ratio (9), we have

$$\Omega_{ls} = \frac{1}{n_g}\Omega_g \tag{54}$$

$$T_{hs} = \frac{1}{n_g}T_{ls} \tag{55}$$

And from (6) (8) and using (54), we can found

$$\dot{\Omega}_r = \frac{1}{J_r}(T_a - T_{ls} - K_r\Omega_r) \tag{56}$$

$$\dot{\Omega}_{ls} = \frac{1}{J_g n_g}\left(T_{hs} - K_g\Omega_g - T_{em}\right) \tag{57}$$

By substituting (55) in (57) and (50), (54), (56), (57) in (49), we obtain

$$\begin{aligned}\dot{T}_{ls} = &\left(B_{ls} - \frac{K_{ls}K_r}{J_r}\right)\Omega_r + \frac{1}{n_g}\left(\frac{K_{ls}K_g}{J_g} - B_{ls}\right)\Omega_g \\ &- K_{ls}\left(\frac{J_r + n_g^2 J_g}{n_g^2 J_g J_r}\right)T_{ls} + \frac{K_{ls}}{J_r}T_a + \frac{K_{ls}}{n_g J_g}\end{aligned} \tag{58}$$